Ablation pressure scaling at short laser wavelength

D. Batani, H. Stabile, A. Ravasio, G. Lucchini, F. Strati, and T. Desai
Dipartimento di Fisica "G. Occhialini," Università degli Studi di Milano Bicocca and INFM, Piazza della Scienza 3, 20126 Milano, Italy

J. Ullschmied, E. Krousky, J. Skala, L. Juha, B. Kralikova, M. Pfeifer, Ch. Kadlec, T. Mocek, and A. Präg
Prague Asterix Laser System Research Centre, Za Slovankou 3, 18221 Prague 8, Czech Republic

H. Nishimura and Y. Ochi
Institute of Laser Engineering, Osaka University, 2-6 Yamadaoka, Suita City, Osaka 565-0871, Japan
(Received 20 February 2003; published 31 December 2003)

The ablation pressure at a 0.44-μm laser wavelength has been measured at irradiance up to 2×10^{14} W/cm^2. The diagnostics consisted in the detection of shock breakout from stepped Al targets. By adopting large focal spots and smoothed laser beams, the lateral energy transport and "drilling effects" have been avoided. The measured scaling shows a fair agreement with analytical models.

DOI: 10.1103/PhysRevE.68.067403 PACS number(s): 52.50.Jm, 52.35.Tc, 52.38.Mf

INTRODUCTION

The process of laser ablation of low- and medium-Z targets is fundamental for laser-driven inertial confinement fusion since it is the source of the driving pressure in ablative compression of fusion targets. For this reason, the study of the mass ablation rate and of the generation of ablation pressures have been among the first subjects to be addressed in the context of laser-matter interaction. In particular, such studies focused on establishing the scaling laws vs laser intensity and laser wavelength, to be used as a guide in the selection of laser parameters, in order to obtain the highest hydrodynamic efficiency in laser-driven implosions.

Also, when laser light is incident on solids, a high-density plasma is formed. Light is absorbed only in the region at and below the critical density. The absorbed energy is then transported by thermal conduction from the absorption region to the higher density ablation region. Therefore, mass ablation is closely related to electron thermal conduction, and measurements can give information on the inward heat flux. This gives an additional motivation for studying laser ablation.

It is then not surprising that many theoretical and experimental studies have been carried out over the past 20 years [1–27]. Despite this, there are still some good reasons to study the process of laser ablation today:

(i) First, progress in laser technology and in laser smoothing techniques allow the realization of cleaner experiments. Indeed it turns out that most past studies were done by focusing the laser energy to small focal spots in order to achieve intensities of $10^{13}-10^{15}$ W/cm^2. Thereby, experimental results were affected by two-dimensional (2D) effects (lateral transport of thermal energy, lateral flow of mass).

Even when large spots were used, these were not optically smoothed (the first smoothing technique, random phase plates, was introduced in the 1980s [28]) and were then characterized by the presence of "hot spots" in the intensity profile. The measured ablation rate was therefore dominated by the "drilling effect" connected to the short-scale inhomogeneities.

Moreover, the use of phase zone plate optical smoothing [29–30] (see the next-section) allows a flat-top intensity distribution to be produced. This is important since the ablation parameters in the central flat region of the focal spot can be directly compared to analytical results obtained from 1D models, which by definition assume a spatially uniform intensity. (In this context, recently interesting results have also been obtained at Institute of Laser Engineering with the partial coherent light technique, PCL [31].)

(ii) At the shortest laser wavelengths, there is still some incertitude concerning the scaling vs laser intensity. For instance, measurements at 0.351 μm by Key *et al.* [1] showed a scaling $\approx I^{0.3}$, very different from what predicted by various theoretical models (usually $\approx I^{0.7}$). Indeed such experimental results were dominated by 2D and drilling effects. Also, to our knowledge, data for the 0.44-μm laser ablation of aluminum targets in the range $10^{13}-10^{14}$ W/cm^2 have not been reported. This is important because shorter laser wavelengths (third and fourth harmonics of Nd, as well as other wavelengths from gas lasers) have the advantage of giving higher ablation rate and pressure, and are thereby envisaged as future drivers for inertial confinement fusion direct drive experiment [32].

(iii) Finally, some details are still not clear in the literature concerning the very mechanism of laser ablation. For instance, even recent important reviews [33] report the scaling law

$$P\ (\mathrm{Mbar}) = 8.6(I/10^{14})^{2/3}\lambda^{-2/3}(A/2Z)^{1/3}, \qquad (1)$$

where I is the laser intensity on target in W/cm^2, λ is the laser wavelength in μm, and A and Z are the mass number and the atomic number of the target. This is obtained by considering that laser light is absorbed at the plasma critical layer.

In reality, the mass ablation rate scaling should also include a time dependence. Indeed the plasma corona size becomes larger during the interaction, and the distance between the absorption region and the ablation surface ($n_e \approx$ solid material) increases with time. This brings to a decoupling of the laser beam from the target and, as a result, the energy

from the laser is absorbed in the plasma corona (delocalized absorption) and the mass absorption rate decreases with time. In particular it is found that the shock pressure is related to laser and target parameters by [34]

$$P\ (\mathrm{Mbar}) = 11.6(I/10^{14})^{3/4}\lambda^{-1/4}(A/2Z)^{7/16}(Z^{*}t/3.5)^{-1/8} \tag{2}$$

where the time t is in ns. As with the previous scaling law (1), pressure strongly depends on laser parameters and only weakly on the material. The decrease in time of ablation pressure, even for constant laser irradiation, was first described by Caruso and Gratton [35] and later by Mora [34]. The difference between delocalized absorption and localized (at critical density) models is discussed in detail by Meyer *et al.* [14].

In order to address questions (i), (ii), and (iii), we performed an experiment at the PALS laboratory, using irradiation at $\lambda = 0.44\ \mu$m [36]. The high laser energy per shot (up to a maximum of 400 J) allowed us to obtain laser intensities up to 2×10^{14} W/cm^2 using relatively large focal spots (diameter 400 μm) and avoiding 2D effects. Also we adopted laser beam-smoothing in order to avoid the ''drilling effect'' from hot spots [25]. Our results show a scaling vs laser intensity which is quite close to the theoretical prediction, and gives some evidence for the mechanism of delocalized absorption.

In the past, several experimental techniques have been used in order to measure the mass ablation rate and pressure. These include the measurement of ablation thickness using time resolved x-ray spectroscopy [3,8], recoil momentum measurements [4], layered target burn trough measurements [2], time resolved x-ray radiography [1], ballistic pendula [14], Faraday cups and plasma energy calorimeters [12], and shock velocity measurements [5,6]. Here we follow the last experimental method, taking advantage of the recent advancement in the generation of high quality shocks and in the measurements of shock velocities with stepped targets [37–39]. As compared to other methods, this is a quite direct measurement of ablation pressure, and less prone to 2D effects [since we measure shock velocity in the central region of the focal spot where shock dynamics is practically 1D thanks to the use of phase zone plates (PZPs), and since the measurement takes place at very early times].

EXPERIMENTAL SETUP

The experiment was performed with the iodine laser of Prague Asterix Laser System (PALS), which delivers a single beam, 29 cm in diameter, with a typical energy of 250 J per pulse at 0.44 μm. The laser pulse is gaussian in time with a full width at half maximum (FWHM) of 450 ps. The schematic experimental setup is shown in Fig. 1.

The focusing lens had a focal length $f = 600$ mm ($f/2$ aperture). A blue filter before the entrance window did cut ω and 2ω light. The diagnostics used to detect the shock breakout from the target rear face consisted in a pair of lenses imaging the rear face onto the slit of a streak camera (Hamamatsu C7700 with an S-1 photocathode). The first one was a complex $f/2$ objective, with $f = 100$ mm, producing a

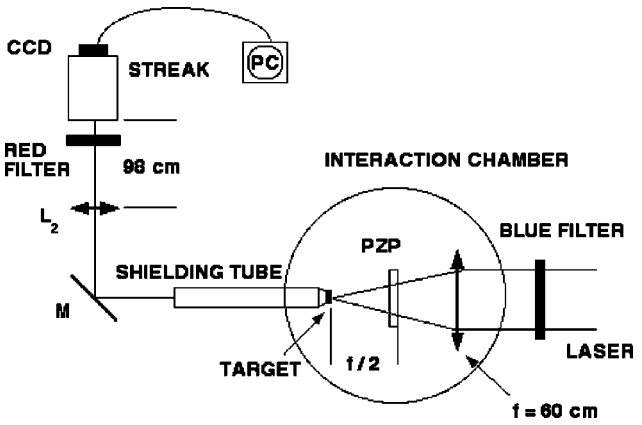

FIG. 1. Experimental setup at PALS.

parallel beam between the two lenses. A protection tube (Fig. 1) was used to shield the diagnostic light path from scattered laser light. A red filter RG60 before the streak camera cut out any 3ω light. The second lens had $f = 98$ cm, giving a total optical magnification $M = 9.8$. The spatial resolution, measured on the CCD placed after the streak by imaging a suitable grid (90-μm pitch), was 2.6 μm/pixel. The CCD had 512×512 pixel and 16 bits dynamic range. The obtained temporal resolution was 3.22 ps/pixel.

Stepped targets were made of lathe machining of bulk aluminum at General Atomics. The base was $\approx 8\ \mu$m, and the step thickness was $\approx 8{,}5\ \mu$m. Al was chosen because its behavior at high pressure is well known, making it a typical reference material for laser-shock experiments.

The primary condition of producing high quality flat shocks imposed the use of PZPs [29,30]. Since, for technical reasons, it was not possible to produce a PZP with the full size of the laser beam, we designed a smaller PZP to be placed at $f/2$ from target. The design had Fresnel lenses of 1-cm diameter, which implies that 225 Fresnel lenses are covered by the laser beam. The characteristics of our optical system (PZP + focusing lens) were such that the focal spot had 400-μm FWHM, with a 250-μm flat region in the center, corresponding to intensities up to 2×10^{14} W/cm^2.

In reality the intensity profile produced by PZPs is not really flat but characterized by small scale length speckles (of typical dimension less than 10 microns). However, small speckles are rapidly washed away by thermal smoothing [40], so they are not expected to influence our measurements. In any case the spatial and temporal resolution of our diagnostics is not sufficient to see such effects. The effects of speckles on shock breakout was observed in Ref. [41] by using a diagnostics with higher space and time resolution. However, it was not large, inducing local differences in shock breakout time of the order of 10 ps, which does not appreciably influence our measurement of shock velocity (which is determined by a shock transit time in the step of the order of 1 nsec).

RESULTS AND DISCUSSION

Figure 2 shows a streak image of shock breakout from an Al stepped target. The time delay between the breakout at the

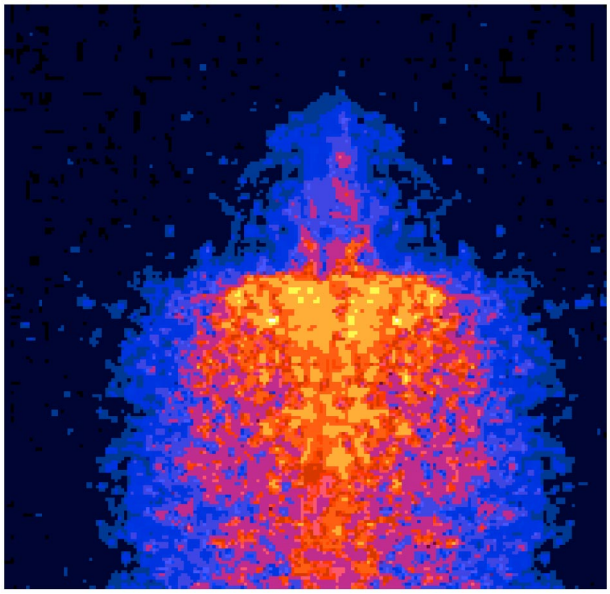

FIG. 2. Shock breakout image from an Al target for laser energy $E_L = 108$ J. The dimensions of the images are 1.69 ns×1300 μm. Times flows up to down. The time delay between base and step is $\Delta t = 267$ ps giving a shock velocity $D = 31.84$ μm/ns

base and at the step gives the average shock velocity in the step. From shock velocity we determine the shock pressure using the Hugoniot data for Al from the Sesame tables [42]. Such a shock pressure is the pressure produced by the laser beam on the irradiation side, i.e., the ablation pressure.

The method works if the shock is stationary, and we designed the targets to get a stationary shock in the step. This can be addressed by using hydrodynamics simulations or analytical models [39,43] which approximate the Gaussian with a trapezoidal time shape.

Typical errors were calculated by considering the error on target thickness (including the surface roughness), the streak camera resolution, as determined by the time window (1.69 nsec) and the slit size (115 μm), and the error in data reading. The error on shock velocity D was then propagated, giving a $\pm 20\%$ error bar on pressure.

The laser intensity on target is obtained by measuring the laser energy shot by shot (through a calibrated reflection from the entrance window of the chamber) and includes the losses (about 20%) due to the use of PZPs [29,30]. Also, it is calculated taking into account the flat-top intensity profile, i.e., it corresponds to the effective intensity in the central region of the focal spot. As for the time dependence, the x axis in Fig. 3 shows the time-averaged intensity over the laser pulse duration.

Figure 3 summarizes our experimental results for ablation pressure vs laser intensity on target. It also shows two theoretical curves corresponding to the law given by Mora, and to the law

$$P\ (\mathrm{Mbar}) = 12(I/10^{14})^{2/3}\lambda^{-2/3}(A/2Z)^{1/3}. \tag{3}$$

This corresponds to Eq. (1) except for the factor 12, which is what was originally derived theoretically [16]. The

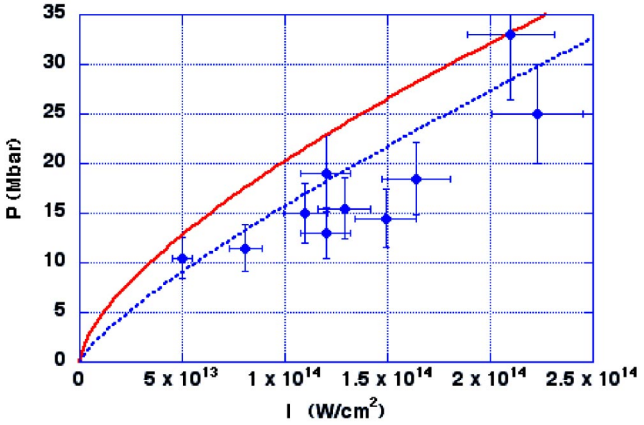

FIG. 3. Our experimental results (dots) with scaling laws for absorption at the critical density [16] [continuous line, Eq. (3)], and to delocalized absorption [34] [dotted line, Eq. (2)].

interpolation of experimental data with Mora's law requires some care. Indeed in the case of delocalized absorption the shock pressure (and shock velocity) decrease with time. Hence weaker shocks, produced at lower intensities, travel more slowly in the target and break out later; thereby they have more time to slow down. Shock velocity is measured at shock breakout, but the shock breakout time [the time t to be inserted into Eq. (2)] is different for low and high laser intensities.

In order to take this effect into account, we write that

$$d = \int D(t)dt, \tag{4}$$

where d is the target thickness, and the time integral goes from 0 to the breakout time. The relation between the shock velocity D and the shock pressure P is [44]

$$D = \left(\frac{(\gamma+1)}{2}\frac{P}{\rho_0}\right)^{1/2}, \tag{5}$$

where γ is the adiabatic constant of the material and ρ_0 is the unperturbed target density ($\rho_0 = 2.7$ g/cm^3 for Al). Equations (4) and (5) allow the shock breakout time to be determined, and by inserting then into Eq. (2) we finally get an equation which is formally independent on time, but dependent on target thickness, i.e.,

$$P\ (\mathrm{Mbar}) = 15.36(I/10^{14})^{0.8}\lambda^{-4/15}\rho_0^{-1/15}d^{-2/15}, \tag{6}$$

where d is in μm and where the coefficient was calculated for $A = 27$ and $Z = Z^* = 13$ (however, the dependence on the ionization degree Z^* is practically negligible). Here we simplified the calculation by assuming an "average" thickness $d = (d_{\mathrm{base}} + d_{\mathrm{step}}/2)$. This may be done because the time exponent in Mora's law (0.125) is very small, i.e., the shock decreases quite slowly with time.

As can be seen, our experimental data are more close to Mora's law, as compared with Eq. (3). This concerns not only the values of pressures but also the trend vs. laser intensity. From this point of view, substituting the factor 12

with the factor 8.6, i.e., using Eq. (1) instead of Eq. (3), may be a tentative of fitting the theoretical scaling obtained for localized absorption with experimental data.

A final remark should concern the possible effect of target preheating induced by the x rays produced in the plasma corona. This might induce some target decompression ahead of shock and alter the measurement of shock velocity. In our case we did measure preheating for every laser shot by recording the emission from the target rear side before shock breakout and using a calibration of our emissivity diagnostics. Preheating temperatures of the order of a couple of eV were measured, and, as expected, increased with increasing laser intensity. Also, we could observe the onset of preheating $\approx$200 ps before shock breakout. Such a short time and the low expansion velocity due to the low preheating temperature combined to give a target decompression which did not affect our shock measurements significantly (especially when compared to our quite large error bars).

Also, let us note that a substantial effect of preheating would appear in a deviation from theoretical laws which is related to preheating temperature, i.e., increasing with laser intensity. Our experimental data instead show no sign of such systematic behavior.

CONCLUSIONS

In summary, the laser ablation pressure at 0.44 μm has been measured in planar Al targets at irradiance up to 2×10^{14} W/cm^2. By adopting relatively large focal spots and a smoothed laser beam, the lateral energy transport and the ''drilling effect'' were avoided. The measured scaling shows a fair agreement with available analytical models. These data can also be of interest for an experimental database of ablation pressure scaling for studies of the equation of state (EOS). Indeed laser shocks have recently become an useful tool in high pressure physics and have in particular been used for the realization of EOS experiments [37,38].

ACKNOWLEDGMENTS

Work performed at PALS under EU Contract No. HPRI-CT-1999-00053 Transnational Access to Major Research Infrastructures (ARI) of the Improving Human Potential (IHP) program of the 5th FP. We thank J. Kaae, General Atomics, for target production and C. Danson and D. Pepler, Rutherford Appleton Laboratory, U.K., for the PZP.

[1] M. H. Key *et al.*, Phys. Fluids **23**, 2011 (1983); M. H. Key *et al.*, Phys. Rev. Lett. **45**, 1801 (1979).
[2] H. Nishimura *et al.*, Phys. Rev. A **23**, 2011 (1981).
[3] T. J. Goldsack *et al.*, Opt. Commun. **42**, 55 (1982).
[4] B. Arad *et al.*, J. Appl. Phys. **50**, 6817 (1979).
[5] R. Trainor, H. W. Shaner, J. M. Auerbach, and N. C. Holmes, Phys. Rev. Lett. **42**, 1154 (1979).
[6] L. R. Veeser and J. C. Solem, Phys. Rev. Lett. **40**, 1391 (1978).
[7] B. H. Ripin *et al.*, Phys. Fluids **23**, 1012 (1980).
[8] T. J. Goldsack *et al.*, Phys. Fluids **25**, 1634 (1982).
[9] F. Dahmani and T. Kerdja, Laser Part. Beams **9**, 769 (1991).
[10] W. B. Fechner *et al.*, Phys. Fluids **27**, 1552 (1984).
[11] G. J. Richard *et al.*, Phys. Rev. Lett. **62**, 2687 (1989).
[12] P. D. Gupta and S. R. Kumbhar, J. Appl. Phys. **55**, 120 (1984); P. Gupta *et al.*, Phys. Fluids **30**, 179 (1987).
[13] T. Boehly *et al.*, J. Appl. Phys. **60**, 3840 (1986).
[14] B. Meyer and G. Thiell, Phys. Fluids **27**, 302 (1984).
[15] A. Ng *et al.*, Appl. Phys. Lett. **45**, 1046 (1984).
[16] R. Fabbro *et al.*, Phys. Rev. A **26**, 2289 (1982); R. Fabbro, C. E. Max, and E. Fabre, Phys. Fluids **28**, 2580 (1985); R. Fabbro *et al., ibid.* **28**, 3414 (1985).
[17] H. Pant *et al.*, J. Appl. Phys. **55**, 697 (1984).
[18] J. A. Tarvin *et al.*, Phys. Rev. Lett. **51**, 1355 (1983).
[19] J. Grun *et al.*, Appl. Phys. Lett. **39**, 545 (1981).
[20] J. S. De Groot *et al.*, Phys. Fluids B **4**, 701 (1992).
[21] C. E. Max *et al.*, Phys. Fluids **23**, 1620 (1980).
[22] R. E. Kidder, Nucl. Fusion **14**, 797 (1974).
[23] V. Vovchenko, I. Krasyuk, P. Pashinin, and A. Yu. Semenov, Dokl. Akad. Nauk **338**, 322 (1994) [Phys. Dokl. **39**, 633 (1994)].
[24] F. Dahmani and T. Kerdja, Phys. Fluids B **3**, 1232 (1991).
[25] I. G. Lebo *et al.*, Laser Part. Beams **17**, 753 (1999).
[26] B. Yaakobi *et al.*, Opt. Commun. **39**, 175 (1981).
[27] X. Deng *et al.*, Appl. Opt. **25**, 377 (1986).
[28] Y. Kato *et al.*, Phys. Rev. Lett. **53**, 1057 (1984).
[29] R. M. Stevenson *et al.*, Opt. Lett. **19**, 363 (1994).
[30] M. Koenig *et al.*, Phys. Rev. E **50**, R3314 (1994); D. Batani, C. Bleu, and Th. Lower, Eur. Phys. J. D **19**, 231 (2002).
[31] T. Sakaiya *et al.*, Phys. Rev. Lett. **88**, 145003 (2002), and references therein.
[32] M. Koenig *et al.*, Laser Part. Beams **10**, 573 (1992).
[33] J. Lindl, Phys. Plasmas **2**, 3933 (1995).
[34] P. Mora, Phys. Fluids **25**, 1051 (1982).
[35] A. Caruso and R. Gratton, Plasma Phys. **10**, 867 (1968).
[36] K. Jungwirth *et al.*, Phys. Plasmas **8**, 2495 (2001).
[37] M. Koenig *et al.*, Phys. Rev. Lett. **74**, 2260 (1995).
[38] D. Batani *et al.*, Phys. Rev. B **61**, 9287 (2000).
[39] D. Batani *et al.*, Eur. Phys. J. D **23**, 99 (2003).
[40] D. Batani *et al.*, Phys. Rev. E **62**, 8573 (2000).
[41] A. Benuzzi *et al.*, Phys. Rev. E **60**, R2488 (1999).
[42] SESAME Report on the Los Alamos Equation-of-State library, Report No. LALP-83-4 (T4 Group LANL, Los Alamos, 1983).
[43] D. Batani *et al.*, Phys. Rev. E **63**, 046410 (2001).
[44] Ya. B. Zeldovich and Yu. P. Raizer, *Physics of Shock Waves and High Temperature Hydrodynamic Phenomena* (Academic Press, New York, 1967).